Journal of The Electrochemical Society, **156** (6) H443-H447 (2009)
0013-4651/2009/156(6)/H443/5/$25.00 © The Electrochemical Society

Kinetics of Deposition of Cu Thin Films in Supercritical Carbon Dioxide Solutions from a F-Free Copper(II) β-Diketone Complex

Masahiro Matsubara,[a,z] Michiru Hirose,[a] Kakeru Tamai,[a] Yukihiro Shimogaki,[b,*] and Eiichi Kondoh[a,*]

[a]*Interdisciplinary Graduate School of Medicine and Engineering, University of Yamanashi, Kofu 400-8511, Japan*
[b]*Department of Materials Engineering, The University of Tokyo, Tokyo 113-8656, Japan*

Kinetics of deposition of Cu thin films in supercritical carbon dioxide solutions from copper bis(di-isobutyrylmethanate) $\{Cu[(CH_3)_2CH(CO)CH(CO)CH(CH_3)_2]_2\}$, $Cu(dibm)_2$, a F-free copper(II) complex, via hydrogen reduction were studied. A flow-type reaction system was employed to control each deposition parameter independently and at a constant value. Apparent activation energies for Cu growth were determined for a temperature range of 200–260°C as a function of hydrogen concentration. The determined values varied from 0.35 to 0.63 eV and decreased as hydrogen concentration increased. At a deposition temperature of 200°C, growth rate followed a Langmuir-type dependence against $Cu(dibm)_2$ and hydrogen concentrations, showing first-order dependence at lower concentrations and zero-order dependence at higher concentrations. At a higher deposition temperature of 240°C, no saturation in the growth rate was observed. A Langmuir–Hinshelwood-type growth mechanism was discussed, and a rate equation for growth was proposed, taking into account the temperature dependence of both the rate constant of the rate-determining reaction and adsorption equilibrium constants. The hydrogen concentration dependence of the apparent activation energy for Cu growth was discussed with this rate equation.
 [DOI: 10.1149/1.3110918]

Manuscript submitted October 22, 2008; revised manuscript received March 5, 2009. Published April 10, 2009.

Scaling down of interconnect dimension is one of the most crucial technologies for miniaturization and high density integration of large-scale integrated circuits. This accompanies an increase in the interconnect resistance and a resistance–capacitance delay in signal propagation. To solve these problems, Al (2.50 μΩ cm at 273 K[1]) wiring has been replaced with a low resistivity material of Cu (1.55 μΩ cm at 273 K[1]), especially in logic LSIs.[2] In the damascene vehicle for Cu interconnect manufacturing, Cu is filled, currently electroplated, in pre-engraved trenches or holes in dielectric layers, and excess Cu is removed with chemical mechanical polishing. Therefore, Cu fill is key in the interconnect process, and a novel deposition technology has always been required to meet future continuous scaling-down.

Metal deposition in supercritical carbon dioxide ($scCO_2$) using a metal complex that is dissolved within, sometimes called supercritical fluid chemical deposition (SCFD), is a promising technique as a replacement for the existing electroplating. Filling of Cu in narrow high aspect-ratio features has been successfully demonstrated, as well as for other metals.[3-6] Such an excellent filling capability is attributed to the unique properties of $scCO_2$. $scCO_2$ has a density as high as liquids, diffusivity as high as gases, viscosity as low as gases, solvent ability, and zero surface tension. $scCO_2$ therefore penetrates into small features and delivers dissolved substances therein. The solvent capability of $scCO_2$ also benefits SCFD. $scCO_2$ can clean the substrate surface. Reaction by-products, which usually have a higher solubility than the precursor, are distributed preferentially to the $scCO_2$ environment; therefore, impurities are less incorporated into the deposited films. In addition, $scCO_2$ and unreacted precursor can be collected and recycled, which makes SCFD attractive as an environmentally friendly process.

SCFD has two basic configurations, batch[3,7,8] and flow[9] systems. In a typical batch arrangement, a fixed amount of precursors is charged in a closed reactor, for instance, in an autoclave, together with a substrate and metered CO_2 and H_2. The reactor is then heated to a target temperature accompanying a pressure rise to an expected value. The CO_2 (and H_2) can be supplied to the reactor during this process, whereas the system has no outlet. The arrangement is simple; however, the chemical composition in the reactor varies during the process and therefore is not appropriate for precise control of the deposition process or for a fundamental study of deposition. In addition, the maximum film thickness is limited, because the growth stops when the loaded precursor is exhausted. Furthermore, the reaction by-products accumulate in the reactor, which may result in poor film quality.

To solve these problems, we employed a flow-type SCFD system. In the flow arrangement, CO_2, H_2, and the precursor are continuously supplied at a fixed flow rate, concentration, and pressure. Previously, we studied Cu deposition characteristics and narrow-gap filling capability using copper bis(hexafluoroacetylacetonate) ($\{Cu[(CF_3)(CO)CH(CO)CF_3]_2\}$, $Cu(hfac)_2$, CAS14781-45-4) as a precursor.[9] $Cu(hfac)_2$ is solid and was dissolved to $scCO_2$ by passing $scCO_2$ through a precursor reservoir. Several issues of this system have arisen in the course of the previous study. First, there was a worry that the F atoms involved, $Cu(hfac)_2$, would contaminate the depositing film. F is a reactive and diffusive element and may cause corrosion and erosion or may passivate the film–substrate interface that leads to the deterioration of film adhesion. Second, the maximum thickness is limited by the amount of the precursor loaded into the reservoir. This is crucial in fabricating thick films that are necessary for microelectromechanical system applications. Third, there was a difficulty in the precise control of the precursor concentration, because the dissolution rate is determined by the liquid–solid contact that is less controllable than fluid–fluid mixing. Finally, the outflow from the reservoir is saturated with the precursor, and a small fluctuation in pressure or temperature can easily cause the precipitation of the precursor in the piping.

In the present study, we used copper bis(diisobutylmethanate) [bis(2,6-dimethyl-3,5-heptanedionato)copper(II), $Cu(dibm)_2$, CAS17653-77-9], a F-free β-diketone. $Cu(dibm)_2$ is solid at ordinary temperatures and pressures and is less soluble to $scCO_2$ than $Cu(hfac)_2$ [$Cu(dibm)_2$ has a solubility of $9.2–88.4 \times 10^{-5}$ mol/L at 40°C and 10.3–34.5 MPa, and $Cu(hfac)_2$ has $2.25–5.69 \times 10^{-3}$ mol/L at 40°C and 10.3–31.0 MPa[10]]. In this study, we did not dissolve $Cu(dibm)_2$ directly into $scCO_2$ and used a $Cu(dibm)_2$-dissolving organic solvent (auxiliary solvent, hereafter) instead. This allowed more detailed study of deposition kinetics of Cu thin-film growth.

Experimental

Figure 1 shows a flow-type SCFD system used in the present study. Liquid CO_2, cooled at 0°C, was pressurized to a pressure above the critical point of CO_2 with a high pressure pump designed

* Electrochemical Society Active Member.
z E-mail: g07dm001@yamanashi.ac.jp

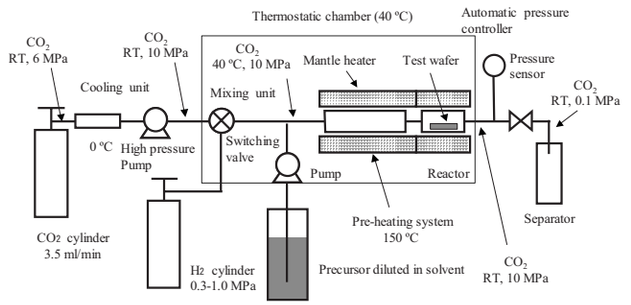

Figure 1. Experimental setup.

for supercritical fluid chromatography (JASCO PU2086). A low pressure (0.1–1 MPa) H_2 gas was added to $scCO_2$ using a gas-mixing unit.[9,11] An auxiliary solvent that is dissolving a precursor was added to $scCO_2$ with a pump for high pressure liquid chromatography (JASCO PU2080) before entering the reactor. The pressure of the system was adjusted with a back-pressure regulator (JASCO SCF Bpg/M) that was placed at the reactor downstream. The $scCO_2$ solution was preheated before the reactor. The gas-mixing unit, reactor, and other related piping and valves were placed in a thermostat oven maintained at 40°C. The internal dimension of the reactor was 60 mm in length, 8 mm in width, and 1 mm in thickness (spacing between substrate and the opposite wall). The substrate was fixed facedown on the reactor wall. Reynolds and Peclet numbers under typical deposition conditions were 150 and 6000, respectively, indicating that the fluid is a laminar plug flow. $Cu(dibm)_2$ was purchased from Kojundo Chemical Laboratory Co., Ltd. (Saitama, Japan) and was used as-is. Substrates used were pieces of Si(100) wafers having a $TaN/Ta/SiO_2$ layer on top. Acetone was used as the auxiliary solvent (Appendix A). Deposition conditions are summarized in Table I. We confirmed, by using another window optical cell, that the $scCO_2$ solutions had a single phase under our experimental conditions, as can be predicted by literature.[12] The surfaces of deposited films were observed with a JOEL JSM6500F field-emission secondary electron microscope (SEM), the film thicknesses were measured with a surface profilometer (DekTak), and θ-2θ X-ray diffraction measurements were performed using Cu Kα emission line.

Results

Basic characteristics of deposited films.— Figure 2 shows SEM photos of film surfaces deposited under typical deposition conditions. The film consists of submicrometer individual grains and exhibits a topography the same as that of chemical-vapor-deposited films.[12,13] The average surface roughnesses, determined using an atomic force microscope, were 19.5 and 30.9 nm for specimens shown in Fig. 2a and b, respectively. The grain size was not precisely studied in these specimens, whereas a typical value of approximately 30 nm was obtained by cross-sectional transmission electron microcopy for a different specimen deposited at 200°C.

The resistivities of the films shown in Fig. 2a and b were 2.1 and 2.0 μΩ cm, respectively. There was a strong tendency for a higher deposition temperature, a higher H_2 concentration, or a higher $Cu(dibm)_2$ concentration to result in a lower resistivity. The average value for all the specimens shown in this paper was 2.42 ± 0.68 μΩ cm, where the second term is the standard deviation. These values were acceptably low for laboratory deposition experiments. There was one exceptionally high value that was not used in the above statistics; however, we confirmed that the exclusion of this data did not affect kinetic analysis shown later.

Table I. Experimental conditions.

Pressure		10 MPa
Reactor temperature		200–280°C
H_2 concentration	(molar ratio to CO_2)	5.63×10^{-3} – 1.53×10^{-2}
$Cu(dibm)_2$ concentration	(molar ratio to CO_2)	6.1×10^{-6} – 2.9×10^{-4}
Molar flow rate	CO_2	77.5×10^{-3} mol/min
	Acetone	4.1×10^{-3} mol/min

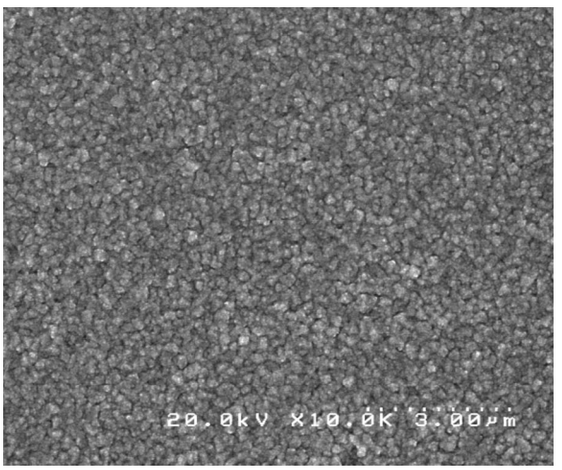

(a)

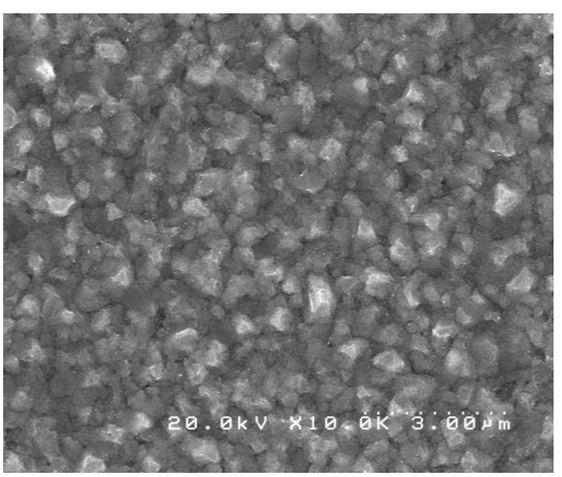

(b)

Figure 2. Scanning electron micrographs of (a) a 260 nm thick Cu film deposited at 200°C and (b) an 890 nm thick film deposited at 240°C. The H_2 and precursor concentrations were 1.53×10^{-2} and 9.72×10^{-5}.

Deposition kinetic data.— Arrhenius plots of growth rate were obtained for different H_2 concentrations of 5.63×10^{-3}, 1.11×10^{-2}, and 1.53×10^{-2} for the deposition temperature range of 200–260°C. The $Cu(dibm)_2$ concentration was fixed at 4.86×10^{-5} (Fig. 3). The Arrhenius plots show a good linear relationship between logarithmic growth rate and reciprocal temperature. The activation energies obtained from the slopes were 0.63 ± 0.10, 0.42 ± 0.06, and 0.35 ± 0.07 eV, showing a decrease with increasing H_2 concentration.

The dependence of growth rate on the $Cu(dibm)_2$ concentration is shown for deposition temperatures of 200 and 240°C in Fig. 4 and 5, respectively. Lines in the figures fit to a Langmuir–Hinshelwood

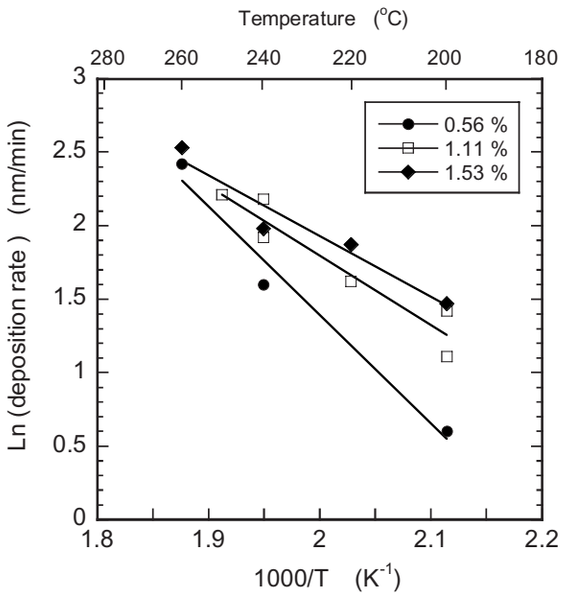

Figure 3. Arrhenius plots of growth rate as a function of H_2 concentration.

rate equation and are discussed later. At 200°C, deposition rate increased with $Cu(dibm)_2$ concentration and saturated at around 1.5×10^{-4}, whereas no clear saturation was observed at 240°C. The maximum growth rate obtained was 35 nm/min. The dependence on H_2 concentration is shown in Fig. 6 and 7. At 200°C, the saturation in growth rate was seen when the $Cu(dibm)_2$ concentration was low $[Cu(dibm)_2 = 4.86 \times 10^{-5}]$. At higher H_2 concentrations, a greater dependence of the growth rate on the $Cu(dibm)_2$ concentration was observed. At 240°C, no saturation was observed and the $Cu(dibm)_2$ concentration dependence was less significant.

Discussion

Surface reactions and apparent rate equation.— The mechanism of Cu chemical vapor deposition from Cu(II) β-diketone complexes has been discussed in past studies.[13-15] In those models proposed, CuL_2 (L is ligand) and H_2 adsorb dissociatively on the surface and Cu deposits through a Langmuir–Hinshelwood reaction between the chemisorbed groups. This reaction accompanies the desorption of an HL by-product being formed from a chemisorbed ligand. Similar Langmuir–Hinshelwood models were employed in the studies of Cu-SCFD.[9,16]

The experimental data presented in this study is more elaborate than the previous SCFD studies and thus is thought to allow for

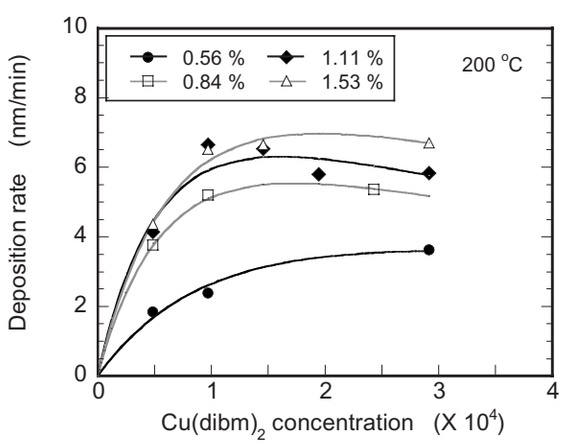

Figure 4. The dependences of growth rate on the precursor concentration at 200°C for different H_2 concentrations. Lines are fits to a Langmuir–Hinshelwood rate equation.

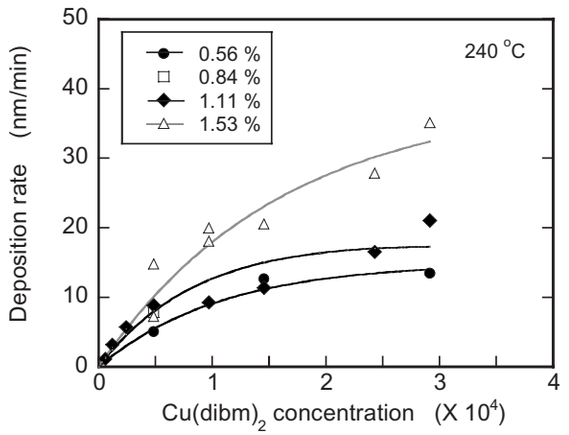

Figure 5. The dependencies of growth rate on the precursor concentration at 240°C for different H_2 concentrations. Lines are fits to a Langmuir–Hinshelwood rate equation.

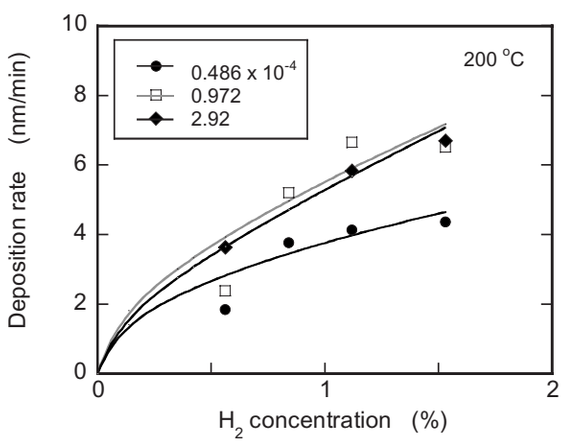

Figure 6. The dependencies of growth rate on H_2 concentration at 200°C for different $Cu(dibm)_2$ concentrations. Lines are fits to a Langmuir–Hinshelwood rate equation.

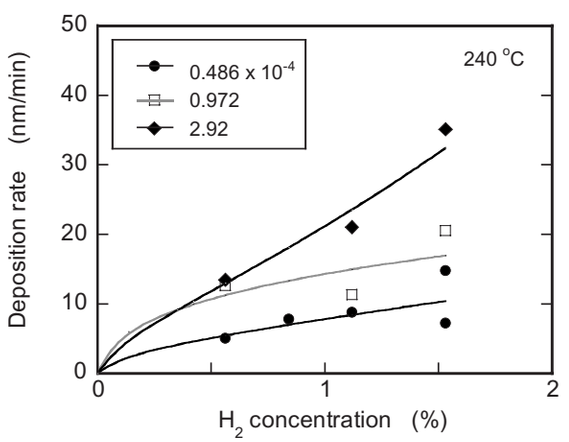

Figure 7. The dependencies of growth rate on H_2 concentration at 240°C for different $Cu(dibm)_2$ concentrations. Lines are fits to a Langmuir–Hinshelwood rate equation.

more extended discussion. Here, we also assume that the rate-determining step of growth is expressed as a Langmuir–Hinshelwood reaction between adsorbed groups. The reaction scheme we propose is as follows

$$CuL_2 + \otimes \leftrightarrow CuL_2 \quad [1]$$

$$H_2 + 2 \oplus \leftrightarrow 2H\oplus \quad [2]$$

$$CuL_2 \otimes + H \oplus \leftrightarrow CuL \otimes + LH\otimes \quad [3]$$

$$CuL \otimes + H \oplus \rightarrow Cu(solid) + LH\otimes \quad [4]$$

$$HL \otimes \leftrightarrow HL + \otimes \quad [5]$$

$\otimes$ and $\oplus$ indicate different adsorption sites, $CuL_2\otimes$ expresses CuL_2 adsorbed to the surface site $\otimes$, and $H\oplus$ is a hydrogen atom that is dissociatively adsorbed to site $\oplus$. Single $\otimes$ and $\oplus$ show vacant adsorption sites.

From the adsorption–desorption equilibrium of reactions 1 and 2, we can easily reduce the equations of the coverage of CuL_2 and H

$$\theta_{CuL_2} = \frac{K_{CuL_2}X_{CuL_2}}{1 + \sqrt{K_{H_2}X_{H_2}} + K_{CuL_2}X_{CuL_2} + \Gamma} \quad [6]$$

$$\theta_H = \frac{\sqrt{K_H X_{H_2}}}{1 + \sqrt{K_{H_2}X_{H_2}} + K_{CuL_2}X_{CuL_2} + \Gamma} \quad [7]$$

where θ_{CuL_2} and θ_H are coverages of CuL_2 and H, X_{CuL_2} and X_{H_2} are molar concentration of CuL_2 and H in the environment, K_{CuL_2} and K_{H_2} are equilibrium constants of reactions 1 and 2, and Γ is a term that involves the contribution of the other species, respectively. Reaction 3 is the rate-determining step, and its reaction rate, r, is written as

$$r = k\theta_{CuL_2}\theta_H = k\frac{\sqrt{K_{H_2}X_{H_2}}K_{CuL_2}X_{CuL_2}}{(1 + \sqrt{K_{H_2}X_{H_2}} + K_{CuL_2}X_{CuL_2})^2} \quad [8]$$

where k is a rate constant and we set $\Gamma = 0$, as discussed later.

We take stepwise analytical approaches to examine the validity of Eq. 8. First, a fitting curve was determined by taking X_{CuL_2} as a variable for fixed X_{H_2} and temperature. This procedure is documented in Appendix B. We confirmed excellent agreement of Eq. 8 with experimental data, as shown shortly after. Next, we applied a nonlinear fitting of Eq. 3 to all data sets and obtained temperature dependencies of k, K_{CuL_2}, and K_{H_2}.

Curves in Fig. 4 and 5 were fittings obtained as a function of $Cu(dibm)_2$ concentration, X_{CuL_2}, for each different H_2 concentration, X_{H_2}. We can see a good agreement with the experimental data (shown by symbols). Likewise, fitting curves plotted as a function of H_2 concentration show fairly good agreement (Fig. 6 and 7). From these facts, we concluded that CuL_2 adsorbs nondissociatively and the growth rate has 1/2 and 1st order against θ_H and θ_{CuL_2}, respectively. It is argued that such a good agreement was never obtained when the other reaction orders were assumed. As stated above, it is a common belief in the chemistry of vapor deposition that the surface dissociation of CuL_2 occurs easily.[13-15] The same mechanism was employed in previous Cu-SCFD works.[9,16] A major difference of the present study from those studies is the use of the auxiliary solvent. We presume that a certain mechanism of stabilization of adsorbed precursors works in the solution of $scCO_2$ and acetone under the presence of H_2. This is an interesting topic in view of sorption, catalytic reactions, and phase separation; however, it is too much beyond the scope of this work and should be left for future consideration.

Now we can safely extend Eq. 8 to all the data sets. Deposition reaction and adsorption are thermally activated processes, and k, K_{CuL_2}, and K_{H_2} have a temperature dependence that follows an expression of $A_0 \exp(-(E/k_B/T))$, where A_0 is a pre-exponential factor, E is an activation energy or enthalpy, k_B is the Boltzmann constant, and T is absolute temperature. By substituting this relationship to Eq. 3 and by applying the equation to all the data set, we obtained the nonlinear fitting equation

$$r = 9.78 \times 10^8 \exp\left(-\frac{3990}{T}\right) \times \frac{\left[63.4 \exp\left(\frac{1850}{T}\right)X_{CuL_2}\right]\sqrt{4040 \exp\left(-\frac{6250}{T}\right)X_{H_2}}}{\left[1 + 63.4 \exp\left(\frac{1850}{T}\right)X_{CuL_2} + \sqrt{4040 \exp\left(-\frac{6250}{T}\right)X_{H_2}}\right]^2} \quad [9]$$

It is noted here again that a better fitting was obtained when 1/2 order θ_{H_2} dependence was assumed. We carried out nonlinear fitting equations with a constant value of Γ in Eq. 8. However, the results obtained did not differ much from Eq. 9; the constant was small enough compared to the sum of the other terms in the dominator. This means that the coverages of CuL and LH are small enough. At least, the sum of θ_{CuL_2} and θ_H obtained from Eq. 9 was close to unity and was almost independent of the experimental conditions.

Temperature dependence of adsorption and film growth.— Equation 9 shows that the adsorption equilibrium constant has a formula of $K_{H_2} = 4040 \exp[-(6250/T)]$, so that its heat of adsorption is -0.54 eV (negative). This agrees with common knowledge that chemisorption of H_2 on noble metals does not occur easily at low temperatures and that it has a large heat of adsorption.[17] In contrast, the equilibrium constant of CuL_2, $K_{CuL_2} = 63.4 \exp(1850/T)$, has a positive heat of adsorption (0.16 eV), and therefore CuL_2 adsorbs less as the temperature increases. The heat of adsorption of metal β-diketones has rarely been documented. We presume our value is appropriate with respect to its magnitude for the following reason. Nonfluorinated crystalline metal β-diketones have a high enthalpy of sublimation of about 1–1.5 eV.[18] Due to the solvation effect, unpolymerized or monomer species are expected to have a weaker interaction with a substrate in a solvent ($scCO_2$ in our case), or a small heat of adsorption, which agrees with our data. The rate constant in Eq. 8 is expressed by a formula of $9.78 \times 10^8 \exp[-(3990/T)]$ in Eq. 9. The activation energy of this rate constant is 0.34 eV. We reported an activation energy of 0.45 ± 0.09 eV for the $Cu(hfac)_2$-H_2 chemistry,[9] which moderately agrees with the present data. It is presumed that these values correspond to the activation energy for the rate-determining step of Cu growth from Cu β-diketone complexes.

The effect of temperature on the dependencies of the growth rate on $Cu(dibm)_2$ and H_2 concentrations (Fig. 4-7) can be explained. Either CuL_2 or H_2 exhibits Langmuir-type adsorption and the growth rate is first order for lower concentrations and becomes zero order for high concentrations due to adsorption saturation. This is especially clear at a low temperature of 200°C. Indeed, in Fig. 4, we can see that the growth rate saturates at approximately 1.5×10^{-4}. Under such a condition, we can expect that good conformal deposition in large features, for instance in through silicon vias, can be performed. On the contrary, adsorption saturation does not occur at 240°C in the extent of the present experiments. More CuL_2 and H_2 adsorb as the concentrations increase, and high growth rates were obtained.

Conclusions

We studied deposition kinetics of Cu thin film via hydrogen reduction of $Cu(dibm)_2$ in $scCO_2$ solutions. The activation energies for growth increased from 0.35 to 0.65 eV as the H_2 concentration decreased from 1.53×10^{-2} to 5.63×10^{-3} for the temperature range of 200–260°C. Generally, growth rate increased as $Cu(dibm)_2$

and H_2 concentration increased. At a low deposition temperature of 200°C, the growth rate became zero order at higher $Cu(dibm)_2$ and H_2 concentrations, whereas no significant saturation was observed at 240°C. These results were discussed with a surface reaction mechanism of adsorbed species, and an empirical overall rate equation was obtained, taking into account the temperature dependencies of adsorption equilibrium constants and the rate constant of the rate-determining reaction. In this model, $Cu(dibm)_2$ was supposed to adsorb nondissociatively. This mode can explain the observed dependencies of the activation energies for Cu growth on the H_2 concentration.

University of Yamanashi assisted in meeting the publication costs of this article.

Appendix A
Selection of Auxiliary Solvent

The auxiliary solvent was selected in preliminary experiments. Figure A-1 shows the solubility of $Cu(dibm)_2$ in 1 mL of common solvents. Cyclohexane exhibited the best solubility, and acetone and normal hexane showed approximately half of that. Next, Cu thin films were deposited at 250°C and for 15 min using different auxiliary solvents that dissolve a fixed amount of $Cu(dibm)_2$ in an $scCO_2$–H_2 mixture with a batch reactor. Figure A-2 correlates the Cu film thickness and the film (111) texture, which is expressed as a ratio of the (111) X-ray diffraction intensity against the (200) intensity. It is well known that (111)-textured Cu LSI interconnects show better reliability. Acetone satisfied the largest thickness and (111) texturing, and therefore we chose it as the auxiliary solvent for this work.

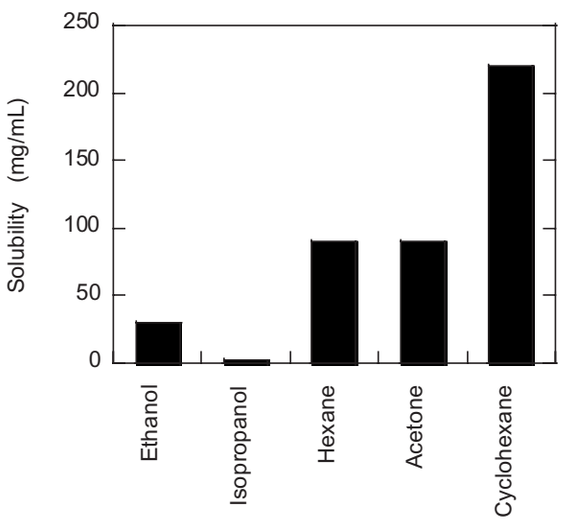

Figure A-1. Solubility of $Cu(dibm)_2$ in common organic solvents.

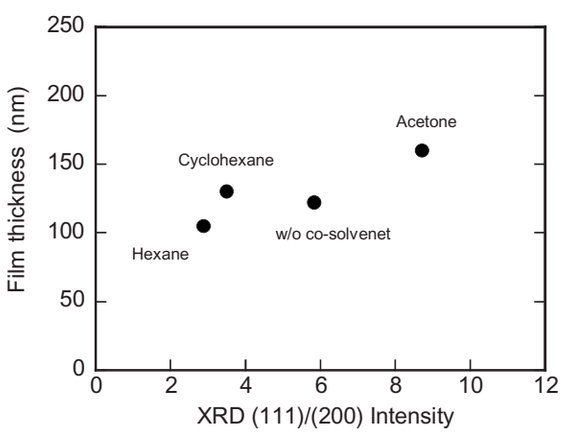

Figure A-2. The effect of kind of auxiliary solvents on (111) texture and film thickness.

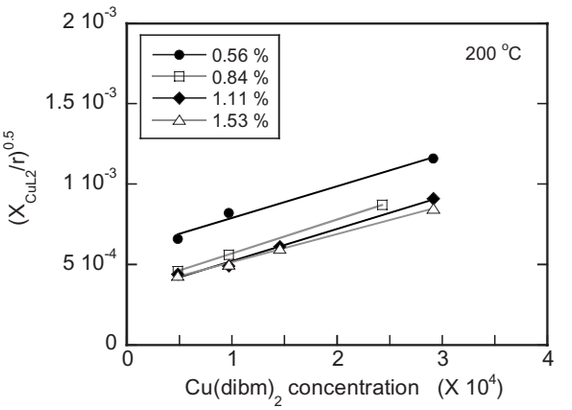

Figure B-1. Langmuir–Hinshelwood plots of the data sets in Fig. 4.

Appendix B
Langmuir–Hinshelwood Plots

The rate of a Langmuir–Hinshelwood reaction can be plotted linearly against the concentration of an adsorbate. For a fixed H_2 concentration, Eq. 3 is transformed to a linear formula for X_{CuL_2}

$$\left(\frac{X_{CuL_2}}{r}\right)^{1/2} = \left(\frac{1}{kK_{CuL_2}\sqrt{K_{H_2}X_{H_2}}}\right)^{1/2}(1+\sqrt{K_{H_2}X_{H_2}}) + \left(\frac{K_{CuL_2}}{k\sqrt{K_{H_2}X_{H_2}}}\right)^{1/2} X_{CuL_2} \quad [B\text{-}1]$$

This formula is equivalent to $(X_{CuL_2}/r)^{1/2} = A + BX_{CuL_2}$, and constants A and B can be determined easily by regression. Then, we obtain a fitting curve of the growth rate as a function of X_{CuL_2} for a fixed H_2 concentration

$$r = \frac{X_{CuL_2}}{(A + BX_{CuL_2})^2} \quad [B\text{-}2]$$

Likewise, we obtain a linear formula for X_{H_2} at a fixed precursor concentration

$$\left(\frac{\sqrt{X_{H_2}}}{r}\right)^{1/2} = \left(\frac{1}{kK_{CuL_2}\sqrt{K_{H_2}X_{H_2}}}\right)^{1/2}(1+K_{CuL_2}X_{CuL_2}) + \left(\frac{\sqrt{K_{H_2}}}{kK_{CuL_2}X_{CuL_2}}\right)^{1/2}\sqrt{X_{H_2}}$$

$$= C + D\sqrt{X_{H_2}} \quad [B\text{-}3]$$

and a fitting curve

$$r = \frac{\sqrt{X_{H_2}}}{(C + D\sqrt{X_{H_2}})^2} \quad [B\text{-}4]$$

Figure B-1 displays a Langmuir–Hinshelwood plot obtained from the data sets in Fig. 4 according to Eq. B-1.

References

1. Y. D. Chen, A. Reisman, I. Turlik, and D. Temple, *CRC Handbook of Electrical Resistivities of Binary Metallic Alloys*, CRC Press, Boca Raton, FL (1983).
2. P. C. Andricacos, C. Uzoh, J. O. Dukovic, J. Horkans, and H. Deligiani, *IBM J. Res. Dev.*, **42**, 567 (1998).
3. E. Kondoh and H. Kato, *Microelectron. Eng.*, **64**, 495 (2002).
4. J. M. Blackburn, D. P. Long, A. Cabanãs, and J. J. Watkins, *Science*, **294**, 141 (2001).
5. E. Kondoh, *Jpn. J. Appl. Phys., Part 1*, **43**, 3928 (2004).
6. T. Momose, M. Sugiyamal, E. Kondoh, and Y. Shimogaki, *Appl. Phys. Express*, **1**, 097002 (2008).
7. J. M. Blackburn, D. P. Long, and J. J. Watkins, *Chem. Mater.*, **12**, 2625 (2000).
8. E. Kondoh and K. Shigama, *Thin Solid Films*, **491**, 228 (2005).
9. E. Kondoh and J. Fukuda, *J. Supercrit. Fluids*, **44**, 466 (2008).
10. J. A. Darr and M. Poliakoff, *Chem. Rev. (Washington, D.C.)*, **99**, 495 (1999).
11. Japan published unexamined, 2006-061862.
12. F. Han, Y. Xue, Y. Tian, X. Zhao, and L. Chen, *J. Chem. Eng. Data*, **50**, 36 (2005).
13. D.-H. Kim, R. H. Wentorf, and W. N. Gill, *J. Electrochem. Soc.*, **140**, 3267 (1993).
14. N. S. Borgharkar and G. L. Griffin, *J. Electrochem. Soc.*, **145**, 347 (1998).
15. W. G. Lai, Y. Xie, and G. L. Griffin, *J. Electrochem. Soc.*, **138**, 3499 (1991).
16. Y. Zong and J. J. Watkins, *Chem. Mater.*, **17**, 560 (2005).
17. K. Christmann, *Surf. Sci. Rep.*, **9**, 1 (1993).
18. M. A. V. Ribeiro da Silva, M. J. S. Monte, and J. Huinink, *J. Chem. Thermodyn.*, **27**, 175 (1995).